



Geomorphology of coralligenous reefs offshore southeastern Sicily (Ionian Sea)

Andrea Giulia Varzi, Luca Fallati, Alessandra Savini, Valentina Alice Bracchi, Pietro Bazzicalupo, Antonietta Rosso, Rossana Sanfilippo, Marco Bertolino, Maurizio Muzzupappa & Daniela Basso

To cite this article: Andrea Giulia Varzi, Luca Fallati, Alessandra Savini, Valentina Alice Bracchi, Pietro Bazzicalupo, Antonietta Rosso, Rossana Sanfilippo, Marco Bertolino, Maurizio Muzzupappa & Daniela Basso (2023): Geomorphology of coralligenous reefs offshore southeastern Sicily (Ionian Sea), Journal of Maps, DOI: [10.1080/17445647.2022.2161963](https://doi.org/10.1080/17445647.2022.2161963)

To link to this article: <https://doi.org/10.1080/17445647.2022.2161963>



© 2023 The Author(s). Published by Informa UK Limited, trading as Taylor & Francis Group on behalf of Journal of Maps



[View supplementary material](#)



Published online: 10 Jan 2023.



[Submit your article to this journal](#)



Article views: 103













[View related articles](#)



[View Crossmark data](#)



Geomorphology of coralligenous reefs offshore southeastern Sicily (Ionian Sea)

Andrea Giulia Varzi ^a, Luca Fallati ^a, Alessandra Savini ^a, Valentina Alice Bracchi ^a, Pietro Bazzicalupo ^a, Antonietta Rosso ^b, Rossana Sanfilippo ^b, Marco Bertolino ^c, Maurizio Muzzupappa ^d and Daniela Basso ^a

^aDepartment of Earth and Environmental Sciences (DISAT), University of Milano-Bicocca, Milano, Italy; ^bDepartment of Biological, Geological and Environmental Sciences, University of Catania, Catania, Italy; ^cDepartment of Earth, Environmental and Life Sciences (DISTAV), University of Genoa, Genoa, Italy; ^dDepartment of Mechanical, Energy and Management Engineering, University of Calabria, Arcavacata, Italy

ABSTRACT

Coralligenous (C) include calcareous build-ups of biogenic origin, formed since the Holocene transgression. Peculiar columnar-shaped C outcrops were documented offshore Marzamemi village (SE Sicily, Ionian Sea), although the actual extension and distribution were not assessed. Project 'CRESCIBLUREEF' produced a new, 17 km² high-resolution bathymetric map, leading to good knowledge about their extent in this area. C bioconstructions are largely distributed along two depth ranges 36–42 m and 86–102 m water depth. By coupling the documented uplift rate in this region and the Holocene sea-level curve, we were able to interpret the distribution of C outcrops over terraces. However, additional investigation is required to understand: (1) the role of the inherited continental shelf landscape, in creating a favorable substrate for the settlement and growth of C habitats during the Holocene, and (2) the extent to which C bioconstructions can impact the evolution of present-day continental shelf landforms and landscapes.

ARTICLE HISTORY

Received 30 March 2022
Revised 23 August 2022
Accepted 16 December 2022

KEYWORDS



Calcareous build-ups;
submarine geomorphology;
seascape; sea-level changes;
biogeomorphology;
Mediterranean sea

1. Introduction

Coralligenous (C) habitats consist of calcareous formations of biogenic origin and are a characteristic of subtidal systems located within the Mediterranean Sea (Peres, 1982; Ballesteros, 2006). Calcareous structures are largely composed of encrusting Rhodophyta belonging to the orders Corallinales and Hapalidiales (Ballesteros, 2006). C habitats generally develop on rocky coasts or sandy planes, whether or not stable conditions of temperature, salinity, and currents exist, and in areas where irradiance is reduced to 0.05–3% of surface irradiance (Garrabou & Ballesteros, 2000; Costanzo et al., 2021). The growth of C habitats largely depends on the delicate balance between bioconstruction and bioerosion processes (Sartoretto & Francour, 1997; Garrabou & Ballesteros, 2000; Costanzo et al., 2021), and can easily be altered by environmental changes and stressors such as increased sedimentation, biological invasion, and nutrient enrichment (Balata et al., 2005, 2007; Piazzi et al., 2007, 2011; Costanzo et al., 2021). Since definitions and morphological classifications for C bioconstructions have always been difficult due to their variety and complexity (Riding, 2002), and

since, at present, no unanimous consensus exists within the scientific community, here, when referring to C physical tridimensional structures, the terms reef, build-up, and bioconstructions are equally used as descriptions.

Documented C bioconstructions within the Mediterranean Sea show complex tridimensional structures (Bracchi et al., 2015; Marchese et al., 2020). Remarkable lateral growth is dominant (Bosence, 1985; Di Geronimo et al., 2002), although peculiar columnar-shaped structures have been observed that contain subhorizontal (Sartoretto, 1994; Di Geronimo et al., 2002) or vertical (Di Geronimo et al., 2001, 2002) growth. Within the Mediterranean Sea, the extent and biodiversity of C habitats and their role in the carbon cycle (Ballesteros, 2006; Boudouresque et al., 2015; Ingresso et al., 2018; Costanzo et al., 2020) make them one of the most valuable and important marine habitats. Although these structurally complex bioconstructions provide heterogeneous habitats and suitable substrates for the settlement of a variety of organisms (Boudouresque et al., 2015; Costanzo et al., 2020; Bracchi et al., 2022), approximately 95% of C habitats have not been mapped (Martin et al.,

CONTACT Luca Fallati  luca.fallati@unimib.it  Department of Earth and Environmental Sciences (DISAT), University of Milano-Bicocca, P.zza della Scienza 4, 20126, Milano, Italy

 Supplemental map for this article is available online at <https://doi.org/10.1080/17445647.2022.2161963>

© 2023 The Author(s). Published by Informa UK Limited, trading as Taylor & Francis Group on behalf of Journal of Maps

This is an Open Access article distributed under the terms of the Creative Commons Attribution License (<http://creativecommons.org/licenses/by/4.0/>), which permits unrestricted use, distribution, and reproduction in any medium, provided the original work is properly cited.

2014; De Falco et al., 2022). Due to the fact that these habitats are protected by international conventions such as Habitat Directive 92/43/EEC, the SPA/BIO Protocol, the Barcelona Convention, the Bern Convention, and the European Union 1967/2006 Regulation (Costanzo et al., 2020), knowledge of C habitat distribution is fundamental for management and conservation (De Falco et al., 2022).

Offshore Marzamemi (SE Sicily) at the infra-circalittoral boundary, Di Geronimo et al. (2001, 2002) described intriguing columnar-shaped build-ups made by calcareous algae and subordinate invertebrates. In this area, columns rise from the seafloor and reach a height of approximately 1 m in water depths (w.d.) up to around 40 m, forming a sort of patch-reef subparallel to the coastline. Due to material collected by fishers and a map of the entire Gulf of Noto, produced using data acquired in 1981 (Violanti et al., 1990; Rosso & Sanfilippo, 2009), deeper C bioconstructions have been known for quite some time. However, an accurate mapping of this marine habitat has, to date, not been done (Lo Iacono et al., 2018). The main goal of our study was to create a high-resolution, morpho-bathymetric map for the continental shelf offshore Marzamemi that contained a quantitative description for the distribution and extent of C reefs.

2. Study area

The study area is located offshore Marzamemi village (Figure 1). The area is part of the Hyblean Plateau, the northernmost sector of the Pelagian block, and represents the emerging portion of the NE-SW-oriented bulge of the African foreland (Lentini et al., 1994; Distefano et al., 2021a). The plateau is bounded to the NW by a system of NE-SW trending, NW dipping normal faults, and is flanked by the Gela Basin towards the W (Lentini & Carbone, 2014). Towards the E, the plateau is bordered by the Ragusa-Malta Escarpment, a dominant feature of the Central Mediterranean, which represents a regional system of NW-SE/NNW-SSE oriented extensional faults (Grasso & Lentini, 1982; Grasso & Pedley, 1990; Distefano et al., 2021a) that controls the tectonic evolution of the eastern Sicilian offshore region (Grasso et al., 1992; Distefano et al., 2021a). Eastern Sicily, along with the Calabrian Arc region, is one of the most tectonically active regions of Southern Italy. A regional tectonic uplift began around 0.6 Ma (Westaway, 1993; Tortorici et al., 1995; Catalano et al., 2008) and has been continuous over the entire Holocene, leading to the occurrence of an uplifted paleo-shoreline (Firth et al., 1996; Stewart et al., 1997; De Guidi et al., 2003; Antonioli et al., 2004; Ferranti et al., 2007; Catalano et al., 2008). The area we investigated is characterised by a regional uplift of approximately 0.2 mm/yr

since the Late Pleistocene (see Bianca et al., 1999; Catalano et al., 2008; Lambeck et al., 2011; Pavano et al., 2019; Distefano et al., 2021a). Coupled with eustatic sea level changes, uplift produced the deep entrenchment of rivers on land and marine terracing along the margin.

Stratigraphic succession of the Hyblean Plateau consists of carbonate sediments of Triassic to Quaternary age. Carbonate facies reflect distribution of the following paleogeographic domains: a basin known as the ‘Siracusa Sector’ towards the E and the carbonate shelf of the ‘Ragusa Sector’ towards the W (Distefano et al., 2021a). The study area is included within the Siracusa domain. Using stratigraphic logs of Quaternary deposits located close to the Marzamemi village, Distefano et al. (2021a) produced a detailed geological sketch-map of the area. Succession in the area begins with limestones of the Priolo Formation (Upper Cretaceous) associated with the products of subaerial events. An overlying sedimentary succession of Paleocene-Eocene age then occurs, followed by marls of the Tellaro Formation (Middle to Late Miocene). Pliocene units are represented by Trubi Formation (Early Pliocene) and Late Pliocene marls. The final layer, consisting of Quaternary deposits, is represented by calcarenites of the Marzamemi Formation (Late Pleistocene), Holocene alluvial and lagoon sediments, and present-day beach deposits.

Both subaerial and submerged geomorphological features have revealed evidence for erosional forms cut into carbonate units. The submerged morphologies of sublittoral and inner shelf zones, indeed, resemble characteristics typical of karst depressions (Distefano et al., 2021a, 2021b). Subaerial erosional surfaces over the area mark the height reached by relative sea level during the Late Quaternary coupled with regional uplift. Late Pleistocene marine terraces were approximately 15 m above sea level (Gracia & Gutiérrez, 2002; Distefano et al., 2021a). The following evolution produced sedimentary deposition and transformation of river valleys into progressively infilling (estuary Distefano et al., 2021a, 2021b).

3. Methods

Our study is based on three data sets acquired during June 2021 for the first marine expedition of project ‘CRESCIBLUREEF – Grown in the blue: new technologies for knowledge and conservation of Mediterranean reefs’ (Figure 1(b)). Data acquisition was performed onboard the minor vessel Valerio. Positional data were provided by a Trimble RTK GNSS receiver that was connected, in real-time, to a NTRIP network (Leica SmartNet ItalPoS).

The first data set was collected during a Multibeam Echosounder (MBES) survey using a pole-mounted,

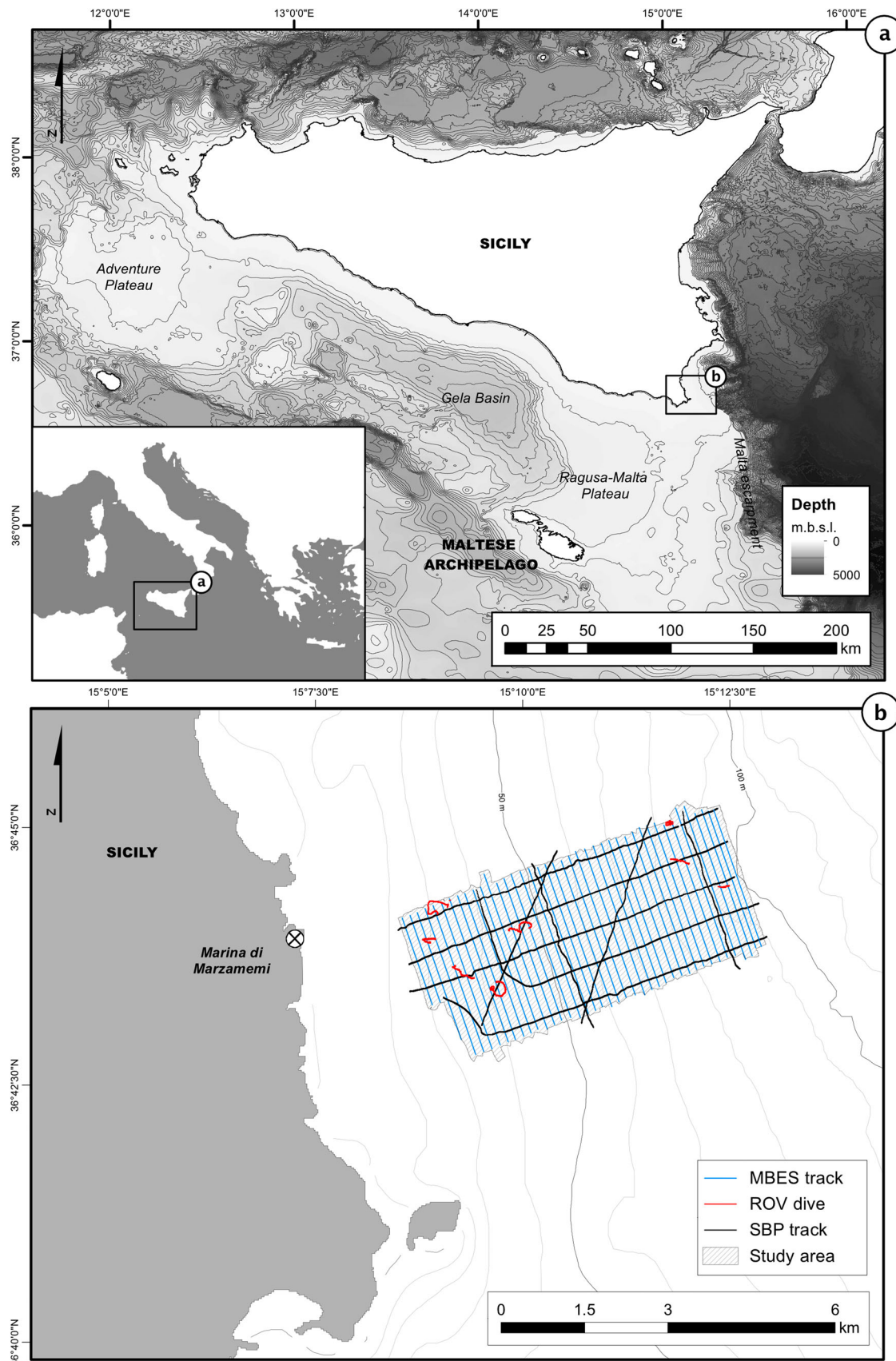


Figure 1. (a) Bathymetric map of the central Mediterranean Sea showing Sicily and the main geomorphological features characterising the area (isobath at 100 m interval). Background bathymetry from EMODnet (<https://www.emodnet-bathymetry.eu/>). (b) Bathymetric map of the southwestern part of Sicily, offshore Marzamemi (isobath at 10 m interval) with indication of the study area, and the location of the MBES tracks, SBP tracks, and ROV dives.

R2-Sonic 2022 system combined with an Integrated Inertial Navigation System (I2NS), which provided accurate and robust georeferencing and motion compensation, and the Sound Velocity Sensor – Valeport miniSVS. Data was collected in 45 tracks (Figure 1(b)) performed at an average speed of 5 knots during three days of field work. The lateral range was kept between 70 and 100 m, with a swath overlap of 10–50%. Approximately 17 km² of seafloor was investigated, with depth ranging from approximately 20 to over 100 m w.d.. A couple of sound velocity profiles were collected each working day, before starting the acquisition in the morning and in the afternoon, using a Sound Velocity Profiler – Valeport miniSVP. The multibeam survey provided both bathymetry and backscatter (BS) data (see Main Map).

The second data set consists of underwater video surveys obtained by using a SEAMOR Steelhead inspection-class Remotely Operated Vehicle (ROV). We identified possible interesting spots on the basis of the MBES data and we planned eight transects (Figure 1(b)) along which visual investigations were performed. Each dive had a duration of about one hour, including the drop-off and drop-on of the ROV. Positional information, with respect to ship position, was obtained with an Ultra-Short Baseline Applied Acoustic Micor Beacon 1200A. Low-definition (LD) videos were acquired using the incorporated camera of the ROV. To obtain high-definition (HD) imagery, we equipped the ROV with a GoPro HERO5. LD and HD videos were used to ground-truth MBES data. The video analysis allowed us to confirm the presence/absence of C and its morphotypes, other than the type of substrate.

The third data set consists of seismic lines, acquired using an Innomar SES-2000 smart, and the SESWIN data acquisition software. Data was collected along 11 tracks (Figure 1(b)). In particular, five were performed following the depth gradient throughout the whole study area, and they were spaced about 600 m to each other to laterally investigate the whole area of interest. Three were conducted perpendicular to those mentioned above, at about 44, 50, and 93 m w.d.. Finally, three were executed following a diagonal course, two with a SW-NE orientation, and one with a NW-SE orientation.

The post-processing of MBES data was performed using QPS Qimera; and included a correction for heading, heave, pitch, and roll. Sound velocity correction process was fulfilled using the sound velocity profiles obtained with the Valeport miniSVP. Corrections for tide were applied considering measurements registered by the Catania station of the Rete Mareografica Nazionale RMN (Istituto Superiore per la Protezione e la Ricerca Ambientale – ISPRA). Finally, soundings were cleaned to remove spikes.

The bathymetric dataset was exported as a 32-bit raster file with a cell size of 3 m. Backscatter data processing was performed using QPS Fledermaus FMGT. Output was exported as an 8-bit raster file with a cell size of 0.3 m.

Mapping operations were conducted using ESRI ArcGIS. Whenever possible, we implemented a semi-automatic approach in order to detect positive morphologies from bathymetric data (Gafeira et al., 2018). The computation of basic land surface parameters, such as the slope gradient and profile curvature, supported the manual mapping of other significant submarine landforms on bathymetry and backscatter data. The processing and interpretation of seismic profiles were performed using the Kingdom Software 2020. RAW data were converted to SEG-Y files using SES Convert software. Seismic data were used to perform seismostratigraphic correlations with published results obtained from seismic reflection surveys conducted offshore Marzamemi (i.e. Distefano et al., 2021a, 2021b).

4. Results

4.1. MBES data

MBES data processing resulted in a Digital Terrain Model (DTM) with a resolution of 3 m (Figure 2). The bathymetric dataset reveals a marked topographic complexity within the shallower region of the study area resulting from positive landforms, which form distinct banks arranged in a rough pattern between 10 and 40 m w.d.. Moving offshore, seafloor complexity drastically decreases, with the exception of deeper areas where the presence of positive morphologies and elongated narrow ridges are evident between 75 and 100 m w.d.. The analysis of DTM-derived local morphometric variables (i.e. slope and curvature) further led to the clear identification of marked breaks in slope (see Main Map), mainly oriented along two perpendicular axes:

- NW-SE, arranged from the shore to the offshore at: (i) 44–48 m, (ii) 62–70 m, (iii) 80–86 m, and (iv) 98–102 m below sea level. The couples of numbers refer to the upper and lower rims of each escarpment, defining the terrace height-drop at the outer rim. The surveyed area results thus to be shaped by four terraces. Additional smaller escarpments clearly denote the presence of two narrow ridges over the third and fourth terraces.
- SW-NE, marking distinct incisions on the seabed in the form of discrete channel-like morphologies. The first one has a mean section of 95 m, and its path yielded two main changes in direction, running a total length of roughly 3 km over the first terrace; the mean vertical relief is of about 2 m. The

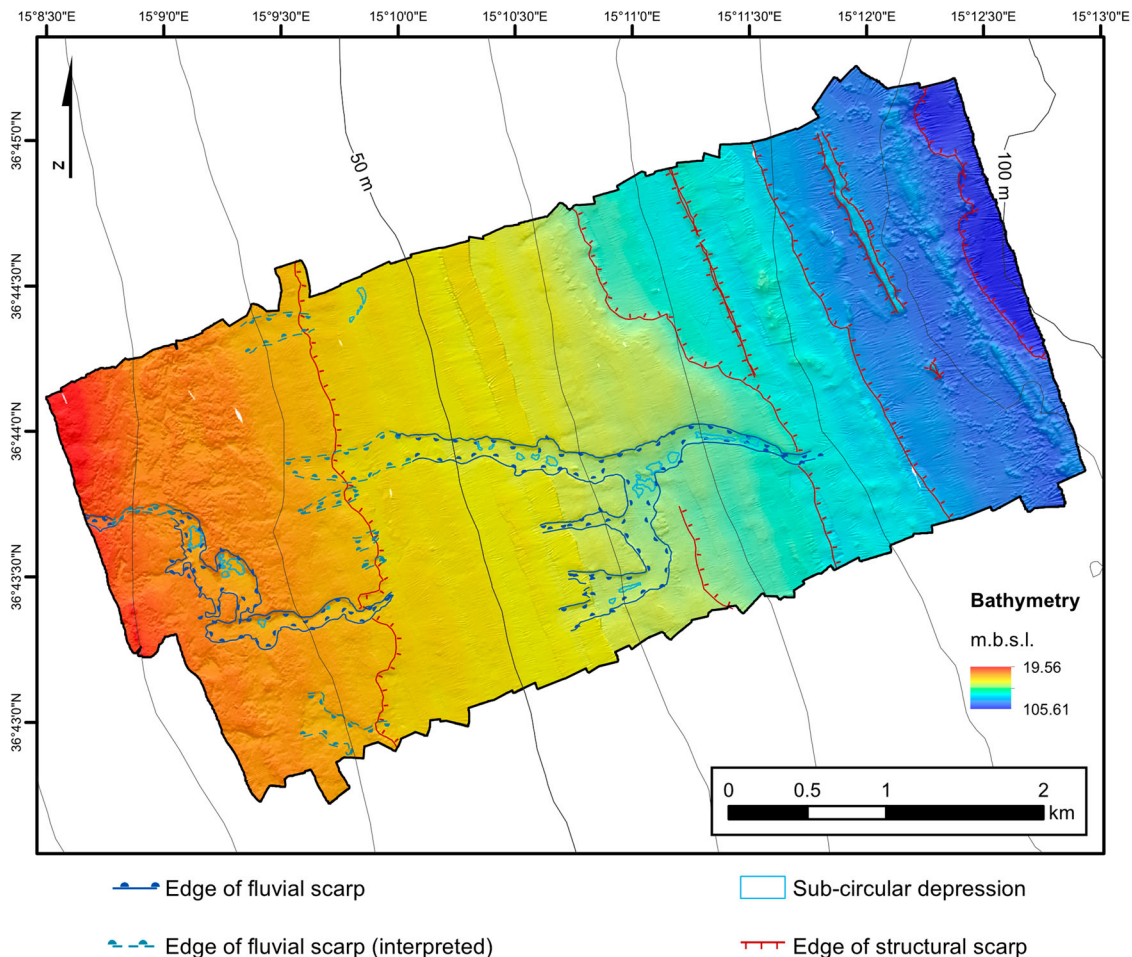


Figure 2. Processed bathymetric data draped on shaded relief map, with a focus on the main geomorphological characteristics that typify the area (isobath at 10 m interval). High-resolution data collected by the MBES survey (R2-Sonic 2022 system) as part of the CRESCIBLUREEF project.

second one has a larger mean section of approximately 145 m, it also crosses the second terrace over a distance of 3 km but follows a more linear path; the mean vertical relief is, again, of about 2 m despite. Both morphologies are characterised by the presence of sub-circular small depressions (between 30 and 60 m in diameter) along the track, with a vertical relief between 0.2 and 0.5 m (Figure 2)

4.2. BS data







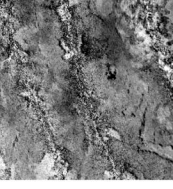


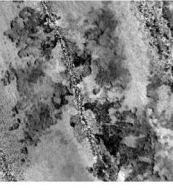
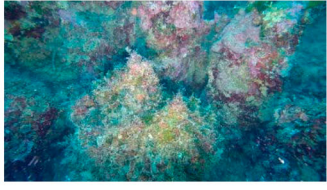

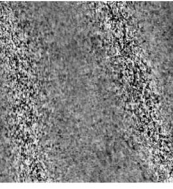


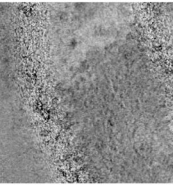
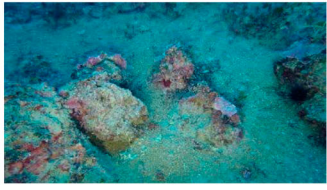
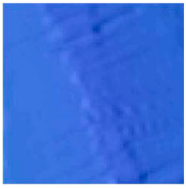
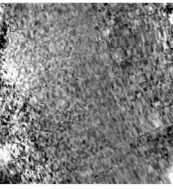

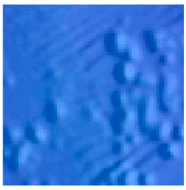
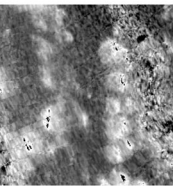

We determined a dependable match between backscatter and topographic complexity. A rough appearance in bathymetric data is, indeed, normally associated with a complex backscattering fabric, while flat areas are defined by a more regular and homogeneous pattern. Since the first terrace is the most complex region, maximum variability in BS is seen throughout this area. The shallower portion is characterised by an intermittent speckled fabric of moderate BS (Table 1(a)). Articulate positive features dominating the area are characterised by a complex fabric of moderate to low BS (Table 1(c)). The

transition between these two patterns is gradual and delimited by a complex fabric of moderate backscatter (Table 1(b)). Besides sub-circular depressions that have an exceptionally low backscatter, flat areas display a more homogeneous pattern of moderate to high intensity (Table 1(d)). A pattern of moderate to high BS typifies the flat seafloor of the second and third terraces. Patches with a dotted pattern of slightly lower signal intensity (Table 1(e)) are locally found over this region. Channels are marked by a more homogeneous BS, although inner sub-circular concavities show much lower intensities. Within the deeper fourth terrace, a high BS intensity (Table 1(g)) typifies the featured mound-like morphologies. The surrounding seafloor displays a homogeneous pattern of low BS (Table 1(f)).

4.3. Visual inspections

ROV videos were crucial for recognising the widespread distribution of C habitats throughout the area, as well as the general layout of various habitats. *Posidonia oceanica* (L.) (Delile, 1813) is abundant up to a depth of about 30 m. Discrete, small build-ups

Table 1. Morpho-acoustic facies identified by combining bathymetric and backscatter data with ROV videos interpretation.

Bathymetry 	Backscatter 	Texture description	Seabed image	Seabed description
		Intermittent speckled fabric of moderate backscatter		Bedrock covered by dense <i>Posidonia oceanica</i> meadows
		Complex fabric of moderate backscatter		Mobile sediment with blocks of C and patches of seagrass
		Complex fabric of moderate to low backscatter		Banks of C of columnar aspect
		Homogeneous pattern of moderate backscatter		Medium to coarse sediment with rhodoliths
		Dotted pattern of moderate backscatter		Small discrete C build-ups surrounded by medium to coarse sediment with rhodoliths
		Homogeneous pattern of low backscatter		Bioturbated fine sediment
		Complex fabric of high backscatter		Blocks of C populated by CWC surrounded by fine sediment

Notes: First and second columns show the bathymetry and backscatter imagery (area of 100 × 100 m). High backscatter is represented by light colours while low backscatter by dark colours. Third column reports backscatter textures description. Representative photographs of the seabed composition and its interpretation are reported as well in the fourth and fifth columns, respectively.

(between 20 and 40 cm in diameter) are scattered over the seafloor among *Posidonia* meadows and are sometimes associated with sparse rhodoliths. Moving offshore, seagrasses become sparser, leaving spaces for positive irregular reefs (e.g. banks) that form

shallow outcrops of approximately 1 m in height. Within the central portion of the surveyed area, C bio-constructions are more sparsely distributed and are not organised in banks. Across the deepest area, C build-ups are visibly larger in both size and height as

compared to the shallower counterparts. An in-depth analysis of ROV videos also allowed the identification of several macro-organisms associated with C build-ups (Table 2).

4.4. Detected habitats

The combination of video and bathymetric data, and the associated backscattering pattern led to the identification of seven distinctive morpho-acoustic facies

(Table 1). We were able to map five main habitats that characterise the surveyed area, and two categories corresponding to mobile substrate, which are ‘Fine sediment’ and ‘Medium to coarse sediment’ (Figure 3). C habitats and morphotypes were categorised by referring to Bracchi et al. (2017). More information about their identification are reported here below:

- *Posidonia oceanica* meadows: Typical *P. oceanica* BS signal was recognised in the shallower region of our

Table 2. List of the species we were able to identify thanks to ROV video surveys.

	IUCN Category		International Legal Instrument	European Legal Instrument	Regional Legal Instrument		
	MED (a)	GLO (b)	CITES (c)	EU Habitats Directive (g)	Protocol SPA/BD (d)	Bern Convention (e)	GFCM Recommendations (f)
Chlorophyta							
<i>Caulerpa cylindracea</i>	NE	NE					
<i>Codium bursa</i>	NE	NE					
<i>Flabellia petiolata</i>	NE	NE					
<i>Halimeda tuna</i>	NE	NE					
Rhodophyta							
<i>Osmundaria volubilis</i>	NE	NE					
Tracheophyta							
<i>Posidonia oceanica</i>	LC	LC			II	I	
Porifera							
<i>Chondrilla nucula</i>	NE	NE					
<i>Phorbas fictitius</i>	NE	NE					
Cnidaria							
<i>Antipathella</i> sp.	NT	NE	II		II		GFCM/43/2019/6 on a establishment of a set of measures to protect vulnerable marine ecosystems formed by cnidarian (coral) communities in the Mediterranean Sea
<i>Dendrophyllia ramea</i>	VU	NE	II		II		
<i>Eunicella cavolini</i>	NT	NE					
<i>Paramuricea macrospina</i>	DD	DD					
Anellida							
<i>Bonellia viridis</i>	NE	NE					
<i>Hermodice carunculata</i>	NE	NE					
Bryozoa							
<i>Margaretta cereoides</i>	NE	NE					
<i>Myriapora truncata</i>	NE	NE					
<i>Reteporella</i> sp.	NE	NE					
Arthropoda							
<i>Calappa granulata</i>	NE	NE					
Echinodermata							
<i>Achantaster</i> sp.	NE	NE					
<i>Astrospartus mediterraneus</i>	NE	NE					
<i>Centrostephanus longispinus</i>	NE	NE		IV	II	II	
<i>Peltaster placenta</i>	NE	NE					
<i>Stylocidaris affinis</i>	NE	NE					
Chordata							
<i>Halocynthia papillosa</i>	NE	NE					
<i>Muraena helena</i>	LC	LC					

Notes: We verified whether such species would have been assessed for the IUCN Red List of Threatened Species both at the Mediterranean (a) and Global (b) level (Vulnerable, VU; Near Threatened, NT; Least Concern, LC; Data Deficient, DD; Not Evaluated, NE) or under other Legal Instruments: (c) CITES, Convention on International Trade in Endangered Species of wild fauna and flora, ratified by all Mediterranean States; in ‘Appendix II – Species’ (see <http://www.cites.org> for full definitions) are listed the taxa not necessarily now threatened with extinction but that may become so unless trade is closely controlled. (d) EU Habitats Directive, Council Directive 92/43/EEC on the Conservation of natural habitats and of wild fauna and flora, it must be implemented in all European States of the Mediterranean. Annex IV – Species of interest to Europe which are in need of strict protection. (e) Protocol SPA/BD, Protocol concerning Specially Protected Area and Biological Diversity in the Mediterranean, ratified by all Mediterranean States (except Greece, Israel, Bosnia and Libya). Annex II – Species that are endangered or threatened. (f) Bern Convention, Convention on the Conservation of European Wildlife and Natural Habitats, ratified by all Mediterranean States of the study, except Algeria, Egypt, Israel, Lebanon. Appendix I – Strictly protected flora species. Appendix II – Strictly protected fauna species. (g) GFCM Recommendations,

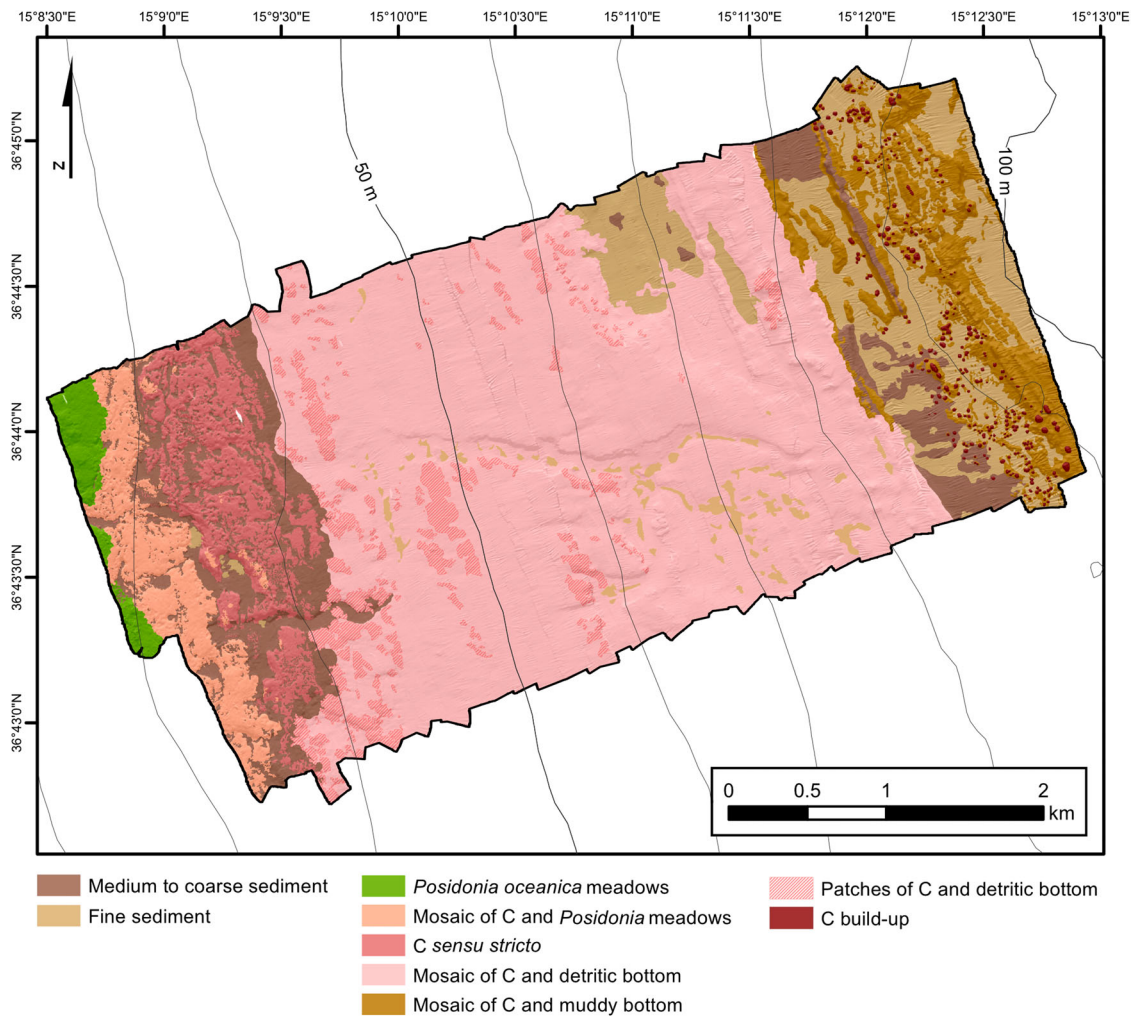


Figure 3. Habitat map of the study area. We identify five major habitats: *Posidonia oceanica* meadows, Mosaic of C and *Posidonia* meadows, C *sensu stricto*, Mosaic of C and detritic bottom, Mosaic of C and muddy bottom. Whenever possible, noticeable areas of C and detritic bottom have been delimited as Patches of C and detritic bottom. Likewise, we mapped recognisable isolated C build-ups in the deep region of the area as C build-up.

study area, up to 30 m w.d.. Here, *P. oceanica* meadows dominate and span 0.27 km² of the seafloor.

- *Mosaic of C and Posidonia meadows*: In the area from 30 to 36 m w.d., typical *P. oceanica* BS signal gradually attenuates. Indeed, ROV videos show that C outcrops begin to be gradually discernible, and *P. oceanica* starts to be less compact. Indeed, we classified a transitional belt that occupies 0.81 km² of the seafloor, to be a mosaic of C habitats and *P. oceanica* meadows.
- *C sensu stricto*: Deeper than 36 m w.d., upon close ROV inspection, *P. oceanica* is not present anymore. Discrete C build-ups are well imaged by ROV. We easily noticed lateral continuity due to the coalescence of C build-ups, especially within the NW region between 36 and 42 m w.d.. In this area, C habitats form hybrid banks with metrical topographic relief, displaying typical cavernous aspects. Intra-areas *sensu* Bracchi et al. (2017) are characterised by medium to coarse sediment. This morphotype represents the transition between isolated build-ups and tabular banks. We classified

these areas, which extend over 0.91 km² of the seafloor from approximately 36 to 42 m w.d., as C *sensu stricto*.

- *Mosaic of C and detritic bottom*: Towards the outer rim of the first terrace and along the entire rim of second and third terraces, large C banks are no longer visible. Nevertheless, ROV dives reveal the presence of discrete, small build-ups often associated with coarse sediments and sparse rhodoliths. Since backscatter signal is similar throughout the whole central part of the investigated area, we, therefore, mapped this area as a mosaic of C habitats and detritic bottom that extends from 42 up to 80 m w.d.. Anyways, small, isolated patches of slightly lower backscatter were recognised throughout this area; ROV videos confirmed in such areas C build-ups are more relevant in respect to the surroundings. Whenever possible, these patches were outlined using another symbology; they span a total area of 0.77 km².
- *Mosaic of C and muddy bottom*: ROV surveys over deeper regions revealed that topographic

complexity, once again, corresponds to the presence of C habitats. Since the mobile substrate surrounding C outcrops is finer in respect to that found in shallower areas, we mapped this habitat, spanning 1.38 km² and extending up to 100 m w.d., as a mosaic of C habitats and muddy bottom. Although these habitats tend to be clustered together, it is often possible to easily discern single build-ups. For this reason, we no longer refer to these C outcrops as banks, but as single discrete build-ups (Bracchi et al., 2017). The sub-circular build-ups in this area have a mean diameter of approximately 20 m and reach heights of approximately 2 m. A total of 295 entities, with a mean area of approximately 365 m², were mapped with a different symbology within this habitat.

5. Discussion

Climate change and tectonic uplift are the dominant forcing mechanisms responsible for the formation of long and narrow terraced landforms in a variety of geomorphic settings. Marine terraces are largely used for reconstructing Quaternary glacial and interglacial climatic phases (Pirazzoli, 1993). With the exception of a few recent studies on the significance of submarine depositional terraces (see Chiocci & Orlando, 1996; Chiocci et al., 2004; De Pippo & Pennetta, 2004; Fraccascia et al., 2013; Pepe et al., 2014; Quartau et al., 2014; Casalbore et al., 2010, 2020), submerged terraced landforms have been poorly investigated (Prampolini et al., 2020), especially with regard to their possible erosive nature as wave-cut or abrasion platforms over outcropping bedrock on the shelf (Bilbao-Lasa et al., 2020; Savini et al., 2020). Throughout the Calabrian Arc region, marine terraces actually represent typical landforms well mapped on-land (Bianca et al., 1999; Catalano & De Guidi, 2003; Tortorici et al., 2003; Catalano et al., 2003, 2008) and associated with main interglacial marine isotope stages (MIS) for the Quaternary period. Based on the distribution for our bathymetric values, submerged terraces were determined to range from: (i) 35–44 m, (ii) 48–62 m, (iii) 70–80 m, and (iv) 86–98 m w.d.. Scarps distinctively mark their outer rims.

By correlating the depth range for such escarpments with the eustatic sea-level curve, some hypotheses can be formulated regarding driving processes and the time of formation. However, due to documented regional uplift (0.2 mm/yr – Distefano et al., 2021a), directly correlating a specific depth value with respect to lowstand periods or transgressive/regressive events is difficult. The scarp delimiting the deepest terrace (98–102 m) offshore actually demands an association with paleo-cliffs likely formed during lowstand periods (MIS 6?). A reasonable hypothesis

is that shallower terraces likely formed between MIS 5 and MIS 2 as wave-cut shore platforms and were likely generated during lowstand periods or transgressive events that promoted erosion. However, further investigations are needed to exactly date their origin. C reefs within the surveyed area are associated with different morphotypes (Bracchi et al., 2017), and their arrangement seems to be correlated with zonation imposed by mapped submerged marine terraces (Figure 4). These exposed, flat bedrock surfaces became available for C settlement and growth at the beginning of the most recent transgressive event (Flandrian) and were favoured by low sedimentation rates.

In agreement with Distefano et al. (2021a), Late Holocene and transgressive sedimentation seem to be concentrated over our two mid-terraces, where considerable C outcrops are not present. In contrast, our analysis indicates that the first and last terraces were likely the most suitable areas for reef development. ROV surveys revealed the presence of megaripples within the surrounding and intra-areas of shallow C bioconstructions, suggesting the presence of moderate currents and, thus, low sedimentation rates. The relationship between C outcrops and *P. oceanica* in defining the lower infralittoral limit within the area is of peculiar concern. In this sense, as the project progresses, further investigations are necessary and are currently being planned. Based on our analysis to date, deep C build-ups appear to be quite different in their morphological expression, suggesting different environmental conditions during settling and growth.

The reefs we investigated, either shallow or deep, are hotspots of biodiversity. ROV videos revealed an abundance of life in association with C habitats, drawing attention to the need for protection and conservation actions. For example, deep C build-ups host anthozoa like *Dendrophyllia ramea* (Linneo, 1758) and *Antipathella* sp., which are both included in the IUCN Red List of Threatened Species at the Mediterranean level, as well as in other legal publications. Since we only performed a preliminary and qualitative analysis, the species recognised from ROV data only represent a snapshot of habitat richness. Given the level of detail in ROV data, we were not able to identify the genus or species of many organisms. Thus, some categories of species may be underestimated. For example, Porifera is known to be a major phyla associated with C habitats (Bertolino et al., 2013; Costa et al., 2019). However, given data quality, we were only able to identify two species.

A seismic-stratigraphic comparison of our data to data reported by Distefano et al. (2021a) suggests that channel-like landforms occupying the central portion of the surveyed area originated as a result of incisions in either Pleistocene or Pliocene carbonatic formations when the seafloor was under subaerial

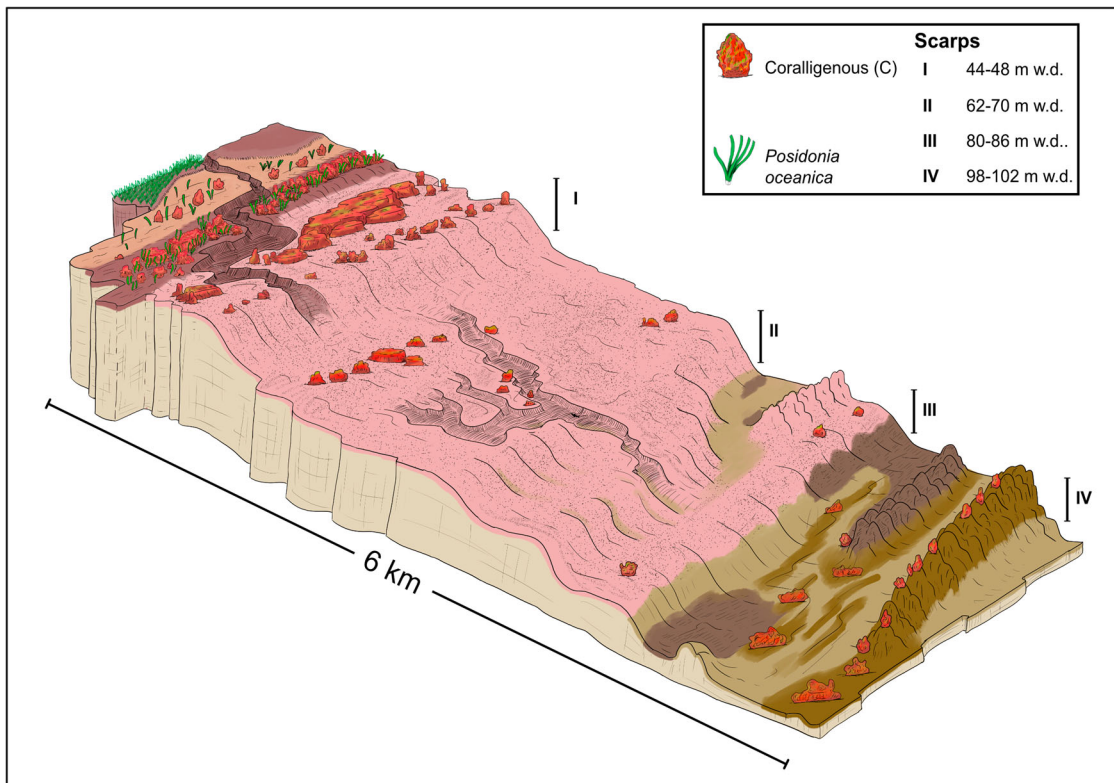


Figure 4. 3D schematic representation of the study area. The four main scarps have been indicated, with a reference to their height. C outcrops are spread all over the area, although as different morphotypes. C reefs result to be more abundant over the shallowest and deepest terraces.

conditions. Due to configuration and, in particular, to small, infilled depressions along its track (relict pot-holes), we believe these formations correspond to a paleo rocky riverbed, which developed as a result of the bedrock karst condition. To better understand the geomorphological layout of the area and the correlation with C settling and distribution, further investigations are required.

6. Conclusions

Data collected within the CRESCIBLUREEF project allowed the realisation of a high-resolution, morpho-bathymetric map of the seafloor off Marzamemi. The Main Map was realized thanks to the interpretation of both bathymetry and backscatter data, together with ROV investigations, that led us to classify the area into five habitats, as well as a geomorphological subdivision based on four distinct marine terraces. C habitats are recognisable throughout the entire surveyed area, and form more evident morphologies over the shallowest and deepest terraces. In particular, the shallow C habitat is in the form of banks, ranging from 30 to 42 m w.d.; deeper C is organised as single build-ups often clustered together, ranging from 86 to 92 m w.d.. Morphological complexity tends to decrease moving offshore. Morphology is highly related to the presence of C reefs, whose formation is likely correlated to late Quaternary lowstand periods

or transgressive/regressive events coupled with the uplifting movements characteristic of this region.

The geomorphological map provides new information regarding extent and characteristics of a major Mediterranean habitat for which knowledge is limited.

Software

The processing of multibeam and backscatter data was done by using QPS Qimera and Fledermaus, respectively. Seismic data were visualised using Kingdom Software 2020. Final maps were produced by using ESRI ArcMap 10.8. Additional graphic operations were done using Affinity Designer. All software was licensed to the University of Milano-Bicocca.

Acknowledgements

This article is a contribution to the project ‘CRESCIBLUREEF – Grown in the blue: new technologies for knowledge and conservation of Mediterranean reefs’. We would like to acknowledge the captain and crew of the survey vessel (M/B Valerio) of Arena Sub S.r.l..

Disclosure statement

No potential conflict of interest was reported by the author(s).

Funding

This work was funded by the Italian Ministry of Research and University – Fondo Integrativo Speciale per la Ricerca (FISR), project FISR2019_04543 CRESCIBLUREEF – Grown in the blue: new technologies for knowledge and conservation of Mediterranean reefs.

ORCID

Andrea Giulia Varzi  <http://orcid.org/0000-0002-4001-2343>

Luca Fallati  <http://orcid.org/0000-0002-5816-6316>

Alessandra Savini  <http://orcid.org/0000-0002-5818-5947>

Valentina Alice Bracchi  <http://orcid.org/0000-0001-9918-7079>

Pietro Bazzicalupo  <http://orcid.org/0000-0002-4011-6230>

Antonietta Rosso  <http://orcid.org/0000-0001-5565-9513>

Rossana Sanfilippo  <http://orcid.org/0000-0001-6154-8027>

Marco Bertolino  <http://orcid.org/0000-0003-3233-303X>

Maurizio Muzzupappa  <http://orcid.org/0000-0002-7717-7571>

Daniela Basso  <http://orcid.org/0000-0002-9352-3569>

References

- Antonoli, F., Dai Pra, G., Segre, A. G., & Sylos Labini, S. (2004). New data on Late Holocene uplift rates in the Messina Strait area, Italy. *Quaternaria Nova*, 8, 45–67.
- Balata, D., Piazzzi, L., & Benedetti-Cecchi, L. (2007). Sediment disturbance and loss of beta diversity on subtidal rocky reefs. *Ecology*, 88(10), 2455–2461. <https://doi.org/10.1890/07-0053.1>
- Balata, D., Piazzzi, L., Cecchi, E., & Cinelli, F. (2005). Variability of Mediterranean coralligenous assemblages subject to local variation in sediment deposition. *Marine Environmental Research*, 60(4), 403–421. <https://doi.org/10.1016/j.marenvres.2004.12.005>
- Ballesteros, E. (2006). Oceanography and marine biology. In *Oceanography and marine biology* (Vol. 44, pp. 135–208). CRC Press. <https://doi.org/10.1201/9781420006391-7>
- Bertolino, M., Cerrano, C., Bavestrello, G., Carella, M., Pansini, M., & Calcinaï, B. (2013). Diversity of Porifera in the Mediterranean coralligenous accretions, with description of a new species. *ZooKeys*, 336, 1–37. <https://doi.org/10.3897/zookeys.336.5139>
- Bianca, M., Monaco, C., Tortorici, L., & Cernobori, L. (1999). Quaternary normal faulting in southeastern Sicily (Italy): A seismic source for the 1693 large earthquake. *Geophysical Journal International*, 139(2), 370–394. <https://doi.org/10.1046/j.1365-246x.1999.00942.x>
- Bilbao-Lasa, P., Jara-Muñoz, J., Pedoja, K., Álvarez, I., Aranburu, A., Iriarte, E., & Galparsoro, I. (2020). Submerged marine terraces identification and an approach for numerical modeling the sequence formation in the Bay of Biscay (Northeastern Iberian Peninsula). *Frontiers in Earth Science*, 8(47). <https://doi.org/10.3389/feart.2020.00047>
- Bosence, D. W. J. (1985). The “Coralligène” of the Mediterranean — a recent analog for tertiary coralline algal limestones. In D. Toomey & M. Nitecki (Eds.), *Paleoalgology* (pp. 216–225). Springer. https://doi.org/10.1007/978-3-642-70355-3_16
- Boudouresque, C. F., Blanfuné, A., Harmelin-Vivien, M., Personnic, S., Ruitton, S., Thibaut, T., & Verlaque, M. (2015). Where seaweed forests meet animal forests: The examples of macroalgae in coral reefs and the Mediterranean coralligenous ecosystem. In S. Rossi, L. Bramanti, L. Gori, & C. Orejas Saco del Valle (Eds.), *Marine animal forests* (pp. 1–28). Springer International Publishing. https://doi.org/10.1007/978-3-319-17001-5_48-1
- Bracchi, V., Savini, A., Marchese, F., Palamara, S., Basso, D., & Corselli, C. (2015). Coralligenous habitat in the Mediterranean Sea: A geomorphological description from remote data. *Italian Journal of Geoscience (Boll. Soc. Geol. It.)*, 134(1), 32–40. <https://doi.org/10.3301/IJG.2014.16>
- Bracchi, V. A., Basso, D., Marchese, F., Corselli, C., & Savini, A. (2017). Coralligenous morphotypes on subhorizontal substrate: A new categorization. *Continental Shelf Research*, 144, 10–20. <https://doi.org/10.1016/j.csr.2017.06.005>
- Bracchi, V. A., Bazzicalupo, P., Fallati, L., Varzi, A. G., Savini, A., Negri, M. P., Rosso, A., Sanfilippo, R., Guido, A., Bertolino, M., Costa, G., de Ponti, E., Leonardi, R., Muzzupappa, M., & Basso, D. (2022). The main builders of Mediterranean coralligenous: 2D and 3D quantitative approaches for its identification. *Frontiers in Earth Science*, 10. <https://doi.org/10.3839/feart.2022.910522>
- Casalbore, D., Falese, F., Martorelli, E., Romagnoli, C., & Chiocci, F. L. (2020). Submarine depositional terraces in the Tyrrhenian Sea as a proxy for paleo-sea level reconstruction: Problems and perspective. *Quaternary International*, 544, 1–11. <https://doi.org/10.1016/j.quaint.2016.07.051>
- Casalbore, D., Romagnoli, C., Chiocci, F., & Frezza, V. (2010). Morpho-sedimentary characteristics of the volcaniclastic apron around Stromboli volcano (Italy). *Marine Geology*, 269(3-4), 132–148. <https://doi.org/10.1016/j.margeo.2010.01.004>
- Catalano, S., & De Guidi, G. (2003). Late Quaternary uplift of northeastern Sicily: Relation with the active normal faulting deformation. *Journal of Geodynamics*, 36(4), 445–467. [https://doi.org/10.1016/S0264-3707\(02\)00035-2](https://doi.org/10.1016/S0264-3707(02)00035-2)
- Catalano, S., De Guidi, G., Monaco, C., Tortorici, G., & Tortorici, L. (2003). Long-term behaviour of the late Quaternary normal faults in the Straits of Messina area (Calabrian arc): structural and morphological constraints. *Quaternary International*, 101, 81–91. [https://doi.org/10.1016/S1040-6182\(02\)00091-5](https://doi.org/10.1016/S1040-6182(02)00091-5)
- Catalano, S., De Guidi, G., Monaco, C., Tortorici, G., & Tortorici, L. (2008). Active faulting and seismicity along the Siculo-Calabrian Rift Zone (Southern Italy). *Tectonophysics*, 453(1-4), 177–192. <https://doi.org/10.1016/j.tecto.2007.05.008>
- Chiocci, F. L., D’Angelo, S., & Romagnoli, C. (2004). Atlas of submerged depositional terraces along the Italian coasts. *Memorie Descrittive Della Carta Geologica D’Italia*, 58.
- Chiocci, F. L., & Orlando, L. (1996). Lowstand terraces on Tyrrhenian Sea steep continental slopes. *Marine Geology*, 134(1-2), 127–143. [https://doi.org/10.1016/0025-3227\(96\)00023-0](https://doi.org/10.1016/0025-3227(96)00023-0)
- Costa, G., Bavestrello, G., Micaroni, V., Pansini, M., Strano, F., & Bertolino, M. (2019). Sponge community variation along the Apulian coasts (Otranto Strait) over a pluri-decennial time span. Does water warming drive a sponge diversity increasing in the Mediterranean Sea? *Journal of the Marine Biological Association of the United Kingdom*, 99(7), 1519–1534. <https://doi.org/10.1017/S0025315419000651>
- Costanzo, L. G., Marletta, G., & Alongi, G. (2020). Assessment of marine litter in the coralligenous habitat

- of a marine protected area along the Ionian coast of Sicily (Central Mediterranean). *Journal of Marine Science and Engineering*, 8(9), 656. <http://dx.doi.org/10.3390/jmse8090656>
- Costanzo, L. G., Marletta, G., & Alongi, G. (2021). Ecological status of coralligenous macroalgal assemblages in the marine protected area (MPA) Isole Ciclopi (Ionian sea). *Plants*, 10(2), 329–315. <https://doi.org/10.3390/plants10020329>
- De Falco, G., Conforti, A., Brambilla, W., Budillon, F., Ceccherelli, G., De Luca, M., Di Martino, G., Guala, I., Innangi, S., Pascucci, V., Piazzì, L., Pireddu, L., Santonastaso, A., Tonielli, R., & Simeone, S. (2022). Coralligenous banks along the western and northern continental shelf of Sardinia Island (Mediterranean Sea). *Journal of Maps*, 1(10), 200–209 <https://doi.org/10.1080/17445647.2021.2020179>
- De Guidi, G., Catalano, S., Monaco, C., & Tortorici, L. (2003). Morphological evidence of Holocene coseismic deformation in the Taormina region (NE Sicily). *Journal of Geodynamics*, 36(1-2), 193–211. [https://doi.org/10.1016/S0264-3707\(03\)00047-4](https://doi.org/10.1016/S0264-3707(03)00047-4)
- De Pippo, T., & Pennetta, M. (2004). Submerged depositional terraces in the Gulf of Policastro (Southern Tyrrhenian sea, Italy). *Memorie Descrittive Della Carta Geologica D'Italia*, 58, 35–38.
- Di Geronimo, I., Di Geronimo, R., Improta, S., Rosso, A., & Sanfilippo, R. (2001). Preliminary observations on a columnar coralline build-up from off SE Sicily. *Biologia Marina Mediterranea*, 8(1), 229–237.
- Di Geronimo, I., Di Geronimo, R., Rosso, A., & Sanfilippo, R. (2002). Structural and taphonomic analysis of a columnar coralline algal build-up from SE Sicily. *Geobios*, 35 (SUPPLEMENT), 86–95. [https://doi.org/10.1016/S0016-6995\(02\)00050-5](https://doi.org/10.1016/S0016-6995(02)00050-5)
- Distefano, S., Gamberi, F., Baldassini, N., & Di Stefano, A. (2021a). Quaternary evolution of coastal plain in response to sea-level changes: Example from south-east Sicily (Southern Italy). *Water*, 13(11), 1524. <https://doi.org/10.3390/w13111524>
- Distefano, S., Gamberi, F., Borzi, L., & Di Stefano, A. (2021b). Quaternary coastal landscape evolution and sea-level rise: An example from south-east Sicily. *Geosciences*, 11(12), 506. <https://doi.org/10.3390/geosciences11120506>
- Ferranti, L., Monaco, C., Antonioli, F., Maschio, L., Kershaw, S., & Verrubbi, V. (2007). The contribution of regional uplift and coseismic slip to the vertical crustal motion in the Messina Straits, southern Italy: Evidence from raised Late Holocene shorelines. *Journal of Geophysical Research*, 112(B6), B06401. <https://doi.org/10.1029/2006JB004473>
- Firth, C., Stewart, I., McGuire, W. J., Kershaw, S., & Vita-Finzi, C. (1996). Coastal elevation changes in eastern Sicily: Implications for volcano instability at Mount Etna. *Geological Society, London, Special Publications*, 110(1), 153–167. <https://doi.org/10.1144/GSL.SP.1996.110.01.12>
- Fraccascia, S., Chiocci, F. L., Scrocca, D., & Falese, F. (2013). Very high-resolution seismic stratigraphy of Pleistocene eustatic minima markers as a tool to reconstruct the tectonic evolution of the northern Latium shelf (Tyrrhenian Sea, Italy). *Geology*, 41(3), 375–378. <https://doi.org/10.1130/G33868.1>
- Gafeira, J., Dolan, M. F. J., & Monteys, X. (2018). Geomorphometric characterization of pockmarks by using a GIS-based semi-automated toolbox. *Geosciences*, 8(5), 154. <https://doi.org/10.3390/geosciences8050154>
- Garrabou, J., & Ballesteros, E. (2000). Growth of *Mesophyllum alternans* and *Lithophyllum frondosum* (Corallinales, Rhodophyta) in the northwestern Mediterranean. *European Journal of Phycology*, 35(1), 1–10. <https://doi.org/10.1080/09670260010001735571>
- Gracia, F. J., & Gutiérrez, M. (2002). Origin and evolution of the gallocanta polje (Iberian range, NE Spain). *Zeitschrift für Geomorphologie*, 46(2), 245–262. <https://doi.org/10.1127/zfg/46/2002/245>
- Grasso, M., & Lentini, F. (1982). Sedimentary and tectonic evolution of the eastern Hyblean Plateau (southeastern Sicily) during late Cretaceous to Quaternary time. *Palaeogeography, Palaeoclimatology, Palaeoecology*, 39 (3-4), 261–280. [https://doi.org/10.1016/0031-0182\(82\)90025-6](https://doi.org/10.1016/0031-0182(82)90025-6)
- Grasso, M., & Pedley, H. M. (1990). Neogene and Quaternary sedimentation patterns in the northwestern Hyblean Plateau (SE Sicily): the effects of a collisional process on a foreland margin. *Rivista Italiana Di Paleontologia e Stratigrafia*, 96(2–3), 219–240.
- Grasso, M., Reuther, C. D., & Tortorici, L. (1992). Neotectonic deformations in SE Sicily: The Ispica fault, evidence of late miocene-pleistocene decoupled wrenching within the central Mediterranean stress regime. *Journal of Geodynamics*, 16(1-2), 135–146. [https://doi.org/10.1016/0264-3707\(92\)90023-L](https://doi.org/10.1016/0264-3707(92)90023-L)
- Ingrosso, G., Abbiati, M., Badalamenti, F., Bavestrello, G., Belmonte, G., Cannas, R., Benedetti-Cecchi, L., Bertolino, M., Bevilacqua, S., Bianchi, C. N., Bo, M., Boscarì, E., Cardone, F., Cattaneo-Vietti, R., Cau, A., Cerrano, C., Chemello, R., Chimienti, G., Congiu, L., ... Boero, F. (2018). Mediterranean bioconstructions along the Italian coast. In C. Sheppard (Ed.), *Advances in marine biology* (Vol. 79, pp. 61–136). Academic Press. <https://doi.org/10.1016/bs.amb.2018.05.001>
- Lambeck, K., Antonioli, F., Anzidei, M., Ferranti, L., Leoni, G., Scicchitano, G., & Silenzi, S. (2011). Sea level change along the Italian coast during the Holocene and projections for the future. *Quaternary International*, 232(1-2), 250–257. <https://doi.org/10.1016/j.quaint.2010.04.026>
- Lentini, F., & Carbone, S. (2014). Geologia della Sicilia - Geology of Sicily. *Memorie Descr. Carta Geologica D'Italia*, 95, 7–414.
- Lentini, F., Carbone, S., & Catalano, S. (1994). Main structural domains of the central Mediterranean region and their Neogene tectonic evolution. *Bollettino Di Geofisica Teorica Ed Applicata*, 36(141–44), 103–125.
- Lo Iacono C, Savini A, Basso D (2018). Cold-Water carbonate bioconstructions. In: Micallef A., Krastel S., Savini A, editors. *Submarine geomorphology*. (pp. 425-455), Springer, ISBN: 425-3-319-57851-4, https://doi.org/10.1007/978-3-319-57852-1_22.
- Marchese, F., Bracchi, V. A., Lisi, G., Basso, D., Corselli, C., & Savini, A. (2020). Assessing fine-scale distribution and volume of Mediterranean algal reefs through terrain analysis of multibeam bathymetric data. A case study in the southern adriatic continental shelf. *Water*, 12(1), 157. <https://doi.org/10.3390/w12010157>
- Martin, C. S., Giannoulaki, M., De Leo, F., Scardi, M., Salomidi, M., Knittweis, L., Pace, M. L., Garofalo, G., Gristina, M., Ballesteros, E., Bavestrello, G., Belluscio, A., Cebrian, E., Gerakaris, V., Pergent, G., Pergent-Martini, C., Schembri, P. J., Terribile, K., Rizzo, L., ... Frascchetti, S. (2014). Coralligenous and maërl habitats: Predictive modelling to identify their spatial distributions

- across the Mediterranean Sea. *Scientific Reports*, 4(1), 5073. <https://doi.org/10.1038/srep05073>
- Pavano, F., Romagnoli, G., Tortorici, G., & Catalano, S. (2019). Morphometric evidences of recent tectonic deformation along the southeastern margin of the Hyblean Plateau (SE-Sicily, Italy). *Geomorphology*, 342, 1–19. <https://doi.org/10.1016/j.geomorph.2019.06.006>
- Pepe, F., Bertotti, G., Ferranti, L., Sacchi, M., Collura, A. M., Passaro, S., & Sulli, A. (2014). Pattern and rate of post-20 ka vertical tectonic motion around the Capo Vaticano Promontory (W Calabria, Italy) based on offshore geomorphological indicators. *Quaternary International*, 332, 85–98. <https://doi.org/10.1016/j.quaint.2013.11.012>
- Peres, J. M. (1982). Major benthic assemblages. *Marine Ecology*, 5.
- Piazzì, L., Balata, D., & Cinelli, F. (2007). Invasions of alien macroalgae in Mediterranean coralligenous assemblages. *Cryptogamie, Algologie*, 28(3), 289–301.
- Piazzì, L., Gennaro, P., & Balata, D. (2011). Effects of nutrient enrichment on macroalgal coralligenous assemblages. *Marine Pollution Bulletin*, 62(8), 1830–1835. <https://doi.org/10.1016/j.marpolbul.2011.05.004>
- Pirazzoli, P. A. (1993). Global sea-level changes and their measurement. *Global and Planetary Change*, 8(3), 135–148. [https://doi.org/10.1016/0921-8181\(93\)90021-F](https://doi.org/10.1016/0921-8181(93)90021-F)
- Prampolini, M., Savini, A., Fogliani, F., & Soldati, M. (2020). Seven good reasons for integrating terrestrial and marine spatial datasets in changing environments. *Water*, 12(8), 2221. <https://doi.org/10.3390/w12082221>
- Quartau, R., Hipólito, A., Romagnoli, C., Casalbore, D., Madeira, J., Tempera, F., Roque, C., & Chiocci, F. L. (2014). The morphology of insular shelves as a key for understanding the geological evolution of volcanic islands: Insights from Terceira Island (Azores). *Geochemistry, Geophysics, Geosystems*, 15(5), 1801–1826. <https://doi.org/10.1002/2014GC005248>
- Riding, R. (2002). Structure and composition of organic reefs and carbonate mud mounds: Concepts and categories. *Earth-Science Reviews*, 58(1-2), 163–231. [https://doi.org/10.1016/S0012-8252\(01\)00089-7](https://doi.org/10.1016/S0012-8252(01)00089-7)
- Rosso, A., & Sanfilippo, R. (2009). *The contribution of Bryozoans y and Serpuloideans p to coralligenous concretions from SE Sicily*. First Mediterranean Symposium on the Coralligenous and Other Calcareous Bioconcretions of the Mediterranean Sea, 1–36. <https://www.researchgate.net/publication/310258686>
- Sartoretto, S. (1994). Structure Et dynamique D’Un nouveau type De bioconstruction a mesophyllum lichenoides (ellis) lemoine (corallinales, rhodophyta). *Comptes Rendus de L’Academie Des Sciences – Serie III*, 317(2), 156–160.
- Sartoretto, S., & Francour, P. (1997). Quantification of bioerosion by sphaerechinus granularis on “coralligene” concretions of the western Mediterranean. *Journal of the Marine Biological Association of the United Kingdom*, 77(2), 565–568. <https://doi.org/10.1017/S0025315400071885>
- Savini, A., Bracchi, V. A., Cammarosano, A., Pennetta, M., & Russo, F. (2020). Terraced landforms onshore and offshore the cileto promontory (south-eastern Tyrrhenian margin) and their significance as Quaternary records of sea level changes. *Water*, 13(4), 566. <https://doi.org/10.3390/w13040566>
- Stewart, I. S., Cundy, A., Kershaw, S., & Firth, C. (1997). Holocene coastal uplift in the Taormina area, northeastern Sicily: Implications for the southern prolongation of the Calabrian seismogenic belt. *Journal of Geodynamics*, 24(1-4), 37–50. [https://doi.org/10.1016/S0264-3707\(97\)00012-4](https://doi.org/10.1016/S0264-3707(97)00012-4)
- Tortorici, G., Bianca, M., De Guidi, G., Monaco, C., & Tortorici, L. (2003). Fault activity and marine terracing in the Capo Vaticano area (southern Calabria) during the Middle-Late Quaternary. *Quaternary International*, 101, 269–278. [https://doi.org/10.1016/S1040-6182\(02\)00107-6](https://doi.org/10.1016/S1040-6182(02)00107-6)
- Tortorici, L., Monaco, C., Tansi, C., & Cocina, O. (1995). Recent and active tectonics in the Calabrian arc (Southern Italy). *Tectonophysics*, 243(1-2), 37–55. [https://doi.org/10.1016/0040-1951\(94\)00190-K](https://doi.org/10.1016/0040-1951(94)00190-K)
- Violanti, V., Di Geronimo, I., & Saccà, R. (1990). Foraminiferal thanatocoenoses from the Gulf of Noto (Southeastern Sicily). *Bollettino del Museo Regionale di Science Naturali Torino, Special*, 773, 799.
- Westaway, R. (1993). Quaternary uplift of southern Italy. *Journal of Geophysical Research: Solid Earth*, 98(B12), 21741–21772. <https://doi.org/10.1029/93JB01566>